American Mineralogist, Volume 82, pages 392–404, 1997

Timing and mechanisms of carbon isotope exchange in granulite-facies calc-silicate boudins, Rauer Group, East Antarctica

IAN CARTWRIGHT,[1] IAN S. BUICK,[2] AND SIMON L. HARLEY[3]

[1]Victorian Institute of Earth and Planetary Sciences, Department of Earth Sciences, Monash University, Clayton, Victoria 3168, Australia
[2]Victorian Institute of Earth and Planetary Sciences, School of Earth Sciences, LaTrobe University, Bundoora, Victoria 3083, Australia
[3]Department of Geology and Geophysics, Grant Institute of Geology, University of Edinburgh, West Mains Road, Edinburgh EH9 3JW, U.K.

ABSTRACT

Mineralogically zoned, decimeter-diameter calc-silicate boudins enclosed within paragneisses from Little Italy Island, Rauer Group, east Antarctica underwent granulite-facies metamorphism (P = 700–900 MPa, T = 840 ± 40 °C) followed by near-isothermal decompression to 200–400 MPa. During decompression several mineral reactions occurred in the presence of a pore fluid ($X_{CO_2} \approx 0.4$). The calc-silicate boudins show a general increase in calcite $\delta^{13}C$ values from core (as low as −17‰) to rim (−9 to −10‰); by contrast, $\delta^{18}O$ values show little variation across the boudins. The $\delta^{13}C$ profiles are similar to those predicted to result from diffusion within a sphere that is surrounded by a homogeneous reservoir. Diffusion of carbon isotopes probably occurred synchronous with the post-peak metamorphic mineral reactions. At that time, centimeter-scale diffusion would have been facilitated by the presence of the fluid, while isotopic exchange between the minerals and the fluid would have been promoted by recrystallization. For metamorphic porosities of $10^{-5} - 10^{-3}$, the $\delta^{13}C$ profiles could have formed in a few thousand to hundreds of thousands of years. Small (millimeter to centimeter) scale variations in $\delta^{13}C$ values that may have been initially present within the boudins would have been homogenized on much shorter timescales than those required to form the profiles. The calculated timescales may reflect the time over which metamorphic recrystallization occurred and a reaction-enhanced porosity was present. Graphite formed locally in the paragneisses only at margins of the boudins probably reflects the local escape of CO_2-bearing fluids from the boudins into relatively low f_{O_2} rocks.

INTRODUCTION

Fluids are important metamorphic and tectonic agents that control the stability of mineral assemblages, cause metasomatism and partial melting, and affect crustal rheologies; hence, documenting fluid-rock interaction is important in understanding crustal processes. The debate about the role of CO_2-rich fluids in producing low aH_2O granulite-facies assemblages (e.g., Newton et al. 1980; Newton 1986) has largely subsided. Many granulite-facies rocks contain mineral assemblages that are too reduced to have been in equilibrium with CO_2-rich fluids, or preserve discontinuities in stable isotope ratios or other geochemical parameters suggesting that they have not experienced significant pervasive fluid flow at any time (e.g., Lamb and Valley 1984; Valley et al. 1990; Cartwright and Valley 1991, 1992; Buick et al. 1993). However, while the peak of metamorphism in many granulite-facies terrains was probably fluid absent, many granulites underwent fluid-rock interaction either before or following the peak of metamorphism (e.g., Corbett and Phillips 1981; Cartwright 1988; Morrison and Valley 1991; Cartwright and Valley 1992; Buick et al. 1994; Cartwright et al. 1993; Buick and Cartwright 1995, 1996; Cartwright and Buick 1995). The timing and duration of these fluid flow episodes and the sources of fluids are often poorly known; hence, there is still a need to document and understand fluid-rock interaction in granulite-facies terrains.

Resetting of stable isotopes commonly occurs during fluid flow; however, it is less clear what the scale of isotopic resetting may be in the absence of fluids. Cartwright and Valley (1992) interpreted discontinuities in $\delta^{18}O$ values of 4–5‰ over <10 cm between anhydrous granulite-facies basic and tonalitic orthogneisses from the Lewisian complex (UK) as indicating that isotopic exchange was very limited in the absence of fluids. By contrast, Todd and Evans (1993) interpreted centimeter-to-decimeter-scale isotopic exchange between granulite-facies marbles and orthogneisses from the Seward Peninsula (USA) as occurring during granulite-facies metamorphism under fluid-absent conditions. The scale over which isotopic resetting occurs is probably controlled by the interplay of

0003–004X/97/0304–0392$05.00

two processes: (1) centimeter-scale transport of isotopic species along grain boundaries or through microfractures that may, at high temperatures, occur at relatively rapid rates even if a fluid is not present; and (2) submillimeter-scale transport of isotopes through individual grains to the grain boundaries.

Here, we examine local fluid-rock interaction between calc-silicate boudins and adjacent pelitic gneisses from the Rauer Group, Antarctica. We propose that diffusion of carbon isotopes took place during a period of mineralogical reactions that occurred during decompression from the metamorphic peak under fluid-present conditions, and that isotopic diffusion was facilitated by both the presence of the fluid and recrystallization.

Local geology

The Rauer Group is a polymetamorphic and polydeformational granulite-facies orthogneiss-dominated terrain in east Antarctica (e.g., Harley 1987, 1988; Harley and Fitzsimons 1991, 1995; Harley et al. 1992, 1995; Fig. 1). There are four main lithological associations: (1) younger, less deformed, felsic to intermediate orthogneisses that locally preserve relict igneous textures; (2) layered paragneisses (including Fe-rich pelites, quartzites, leucocratic gneisses, and calc-silicate rocks); (3) homogeneous felsic to intermediate orthogneisses with strong fabrics that contain boudins and rafts of marble and Mg-rich metapelites; and (4) composite layered felsic and mafic gneisses and minor marble, which are often preserved as rafts within the orthogneisses of association 1. All rocks experienced M3 granulite-facies metamorphism, which occurred at 700–900 MPa and 840 ± 40 °C (Harley 1988; Harley and Buick 1992) and was accompanied by widespread D3 deformation. In areas of low D3 strain, associations 3 and 4 (which occur mainly in the north and northeast of the terrain) preserve evidence of older, pre-M3, granulite-facies tectonic fabrics and mineral assemblages (Harley et al. 1992; Sims et al. 1994). M3 appears to be the only metamorphic event to affect rocks in associations 1 and 2. A variety of ages have been proposed for M3 metamorphism in the Prydz Bay area (e.g., as discussed by Fitzsimons 1997). However, recent SHRIMP U-Pb ages of zircons from orthogneisses and leucosomes in metapelites, Sm-Nd ages from paragneisses, and biotite Ar-Ar ages suggest that metamorphism throughout this area occurred at ~500 Ma (Kinny et al. 1993; Zhao et al. 1992; Hensen and Zhao 1995; Carson et al. 1995). Mineral textures in metapelites, orthogneisses, and calc-silicates indicate that, following the peak of M3, the rocks of the Prydz Bay region underwent near-isothermal decompression through 200–400 MPa while temperatures remained in excess of 750 °C (Harley 1988; Harley and Fitzsimons 1991; Thost et al. 1991; Harley and Buick 1992; Fitzsimons 1997). Systematic differences in ages from isotopic systems with different closure temperatures suggest that decompression and cooling occurred over ~15 Ma (Fitzsimons 1997).

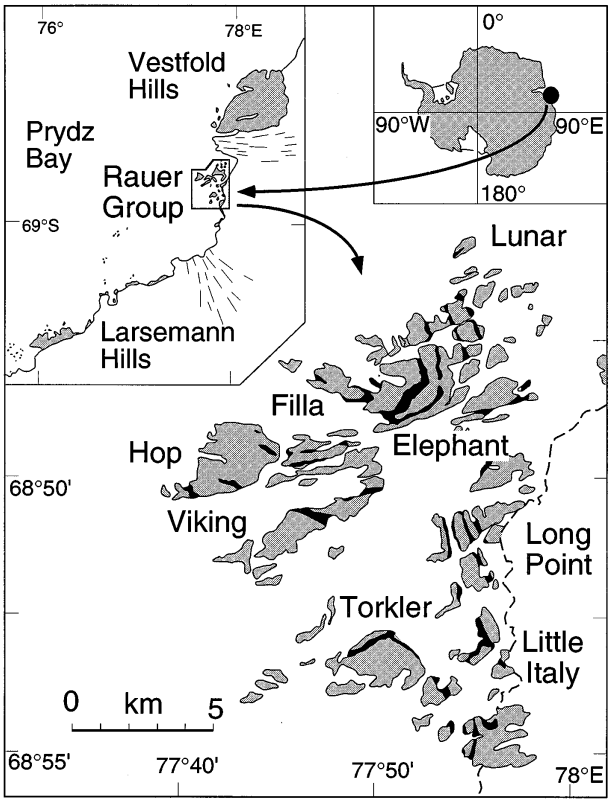

Figure 1. Location map of the Rauer Group in the Prydz Bay region of east Antarctica (after Buick et al. 1993). Main paragneiss occurrences shown black. Samples for this study are from Little Italy Island.

Calc-silicate boudins and adjacent rocks

The calc-silicate boudins from the Rauer Group were described in detail by Harley (1987), Harley and Buick (1992), and Buick et al. (1993), so only brief descriptions are given here. The boudins comprise <1% of the total outcrop and are typically 5–25 cm in diameter with grain sizes of 0.5–1 mm. They are enclosed in pelitic gneisses, and may represent boudinaged layers or the noses of sheath folds elongated parallel to the L3 lineation. The pelites typically contain garnet + sillimanite + quartz + potassium feldspar + plagioclase ± biotite ± orthopyroxene ± ilmenite or rutile. These rocks underwent partial melting during M3 to produce veins and pods of quartz + potassium feldspar + plagioclase + garnet-bearing leucogneiss. Rare mafic rocks contain orthopyroxene + clinopyroxene + plagioclase + garnet assemblages, and also have locally undergone migmatization.

The boudins are concentrically zoned on a centimeter scale (Buick et al. 1993). The earliest mineral assemblages recognized are as follows. The boudin cores commonly contain wollastonite, scapolite, clinopyroxene, grossular-rich garnet, titanite, and calcite or quartz (with calcite- and quartz-bearing assemblages commonly interlayered on a millimeter scale). Surrounding the core is a

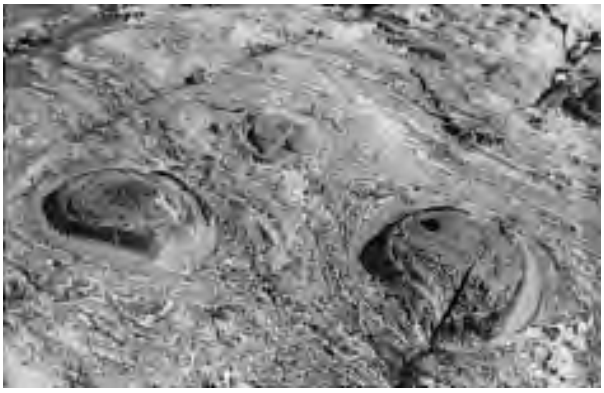

FIGURE 2. Boudins from Little Italy Island enclosed within semipelitic paragneisses. The internal concentric mineralogical zoning is apparent as is the deflection of the S3 fabric around the boudins. Lens cap is 50 mm in diameter.

grandite garnet zone comprising grandite, scapolite, clinopyroxene, titanite, quartz, and local calcite. Outside the grandite garnet zone is a clinopyroxene zone that includes clinopyroxene, quartz, scapolite, titanite, plagioclase, ilmenite and calcite. Across this zone, from the boudin core to the rim, scapolite and titanite disappear and plagioclase and ilmenite increase in abundance. An orthopyroxene zone is developed outside the clinopyroxene zone and comprises orthopyroxene, quartz, plagioclase, ilmenite, and calcite. The outermost zone is an almandine garnet zone that comprises almandine, orthopyroxene, quartz, plagioclase, ilmenite, rutile, magnetite, and locally biotite and calcite. Toward the outer part of this zone, ilmenite and orthopyroxene disappear and rutile and biotite become more abundant. The boundaries between the zones are gradational on a millimeter scale, and individual boudins may show some variation on the mineralogies developed. In particular, the boudins from this study are more carbonate rich than many in the region, and most of the zones contain calcite. The early minerals in the boudins often define the regional syn-peak metamorphic L3 fabric (Harley and Buick 1992).

Buick et al. (1993) proposed that the rocks were originally calcareous layers (limestones or marls). Formation of the wollastonite-bearing assemblages in the boudin cores probably occurred because of the influx of H_2O-rich fluids from surrounding gneisses. The minerals in the boudin cores are aligned in the peak-metamorphic D3 fabrics, implying that fluid infiltration occurred at or before the peak of M3 metamorphism. It is unlikely that fluid flow occurred at the metamorphic peak as water-rich fluids would have caused wholesale melting of the surrounding paragenesses. Hence, fluid flow probably occurred during the prograde stages of M3 or in an earlier unrelated event. Devolatilization during this period of fluid infiltration would have also removed much of the original carbonate from the rocks. The mineral zonation in the boudins reflects chemical zonation. Principally, the boudin cores are richer in Ca, Al, and Mn and poorer in Si, Ti, and Na than the rims. This chemical zonation was probably formed by major element diffusion between the boudins and the surrounding gneisses after the layers were boudinaged during M3 (Buick et al. 1993). The rocks outside the clinopyroxene zone represent modified pelite, while the other zones represent modified calc-silicate. Following the peak of M3 metamorphism, the boudins developed several crosscutting retrograde reaction zones, described below. The pelitic rocks adjacent to the boudins also underwent incipient post-M3 retrogression with biotite rimming garnet and with tremolitic amphibole locally replacing orthopyroxene.

Preliminary stable isotope data presented by Buick et al. (1993) showed that many of the boudin cores have extremely low $\delta^{13}C(Cc)$ values (as low as $-21‰$) and that boudins from the same locality often preserve a variation in $\delta^{13}C(Cc)$ values of several per mil. Given that there is no graphite present in the boudin cores, the low $\delta^{13}C(Cc)$ values probably resulted from decarbonation during the early fluid flow event. Even if some graphite were initially present (and was subsequently oxidized during fluid infiltration), the majority of the carbon would still have resided in carbonate minerals making decarbonation the most likely cause of the low $\delta^{13}C(Cc)$ values.

The boudins from this study come from a 4m $\times$ 7m area from Little Italy Island (Figs. 1 and 2). Continuous samples were collected from the cores of the boudin to the rims and, where possible, into the surrounding pelites. The mineral assemblages of the boudins and the immediately-adjacent pelites, and the reaction textures identified are shown in Table 1. The mineral assemblages are similar to those described by Harley and Buick (1992). In several cases, however, the sequence of reaction zones differs slightly from that reported by Buick et al. (1993). In particular, the grandite zone is often absent. This is probably the result of slight differences in composition between the boudins in this study and those described by Buick et al. (1993). The almandine zone of some of the boudins contains a small amount ($\ll$1%) of graphite that was not previously reported. Texturally, the graphite appears as randomly oriented flakes that are not aligned in the D3 fabrics and which, therefore, probably formed after the peak of M3. In general the pelitic gneisses in this area are not graphite bearing, suggesting that the presence of graphite is related to the boudins. In the almandine zone of boudin 95SH-29, the stable oxide assemblage changes from ilmenite + magnetite near the boudin core to rutile + ilmenite near the rim. Each pair of oxides are in mutual contact and are apparently coexisting. The graphite is concentrated in the ilmenite + magnetite-bearing region.

All boudins were examined under cathodoluminescence (Fig. 3), which helped confirm the textural relationships identified in Table 1. Cathodoluminescence also showed that most of the calcite in these boudins occurs as discrete grains and not as microveins. The only microveins apparent were numerous wollastonite microveins that cut garnet (Fig. 3). The wollastonite probably was

TABLE 1. Mineral assemblages and reaction textures of calc-silicate boudins from Little Italy Island

Zone	Minerals																Reaction
	Cc	Qtz	Wo	Scp	Plg	Ksp	Cpx	Opx	Alm	Grd	Ilm	Tit	Rt	Mt	Bt	Gph	
								92SH-22									
Core	X, I	X	X	X	I							X					C, D, E
Grandite	X	X	I	X, I	X		X			X		X					A, B
Clinopyroxene	X, I	X	I	X	X		X				X	X					D
Orthopyroxene	X	X		X		X	X			X	X				I		
								90SH-25									
Core	X, I	X	X	X	I						X						C, E
Clinopyroxene	X, I	X	I	X	X, I		X					X					C, D
Orthopyroxene	X	X			X			X				X					
Almandine	X	X			X	X		X	X		X, I	X	X		X	X	G
								90SH-26									
Core	X, I	X	X	X	I							X					C, E, F
Grandite	X	X	I	X, I	X		X			X		X					A, B
Clinopyroxene	X	X	I	X	X		X			I		X					
Orthopyroxene	X	X			X			X				X					
Almandine	X	X			X	X		X	X		X, I	X	X		X		
								90SH-29									
Core	X, I	X	X	X	I							X					C, D
Grandite	X	X	I	X, I	X		X			X							A, B
Clinopyroxene	X, I	X	I	X	X		X					X					
Orthopyroxene	X	X			X			X				X					
Almandine	X	X			X	X	X	X	X		X, I	X	X	X	X	X	G, H
								90SH-30E									
Core	X, I	X	X	X	I							X					C, D
Clinopyroxene	X	X	I	X	X, I		X					X					D
Orthopyroxene	X	X		X	X			X				X					D
								90SH-30W									
Core	X, I	X	X	X	I							X					C, D, E
Clinopyroxene	X, I	X	I	X	X, I		X					X					
Orthopyroxene	X	X			X			X				X					

Notes: Calc-silicate reaction textures and inferred CAS reactions. A: Grd replaced by Wo + Scp (Gr + Cc + Qtz = Wo + Me) or (Gr + Qtz + CO_2 = Me + Wo). B: Grd replaced by An + Wo ± Cpx (Gr + Qtz = An + Wo) or (Gr + CO_2 = An + Wo + Cc). C: Scp replaced by Wo + Plg (Me + Qtz = Wo + An + CO_2). D: Scp replaced by fine-grained Plg + Cc (Me = Cc + An). E: Wo replacing Cc (Cc + Qtz = Wo + CO_2). F: Grossular rims Scp + Wo in symplectite (Me + Wo + Cc = Gr + CO_2). Oxide reaction textures and inferred CFTS reactions are as follows. G: Ru replaced by Ilm. H: Tit rimming Ilm adj Cc + Qtz (Qtz + Ilm + Cc = Fs + Tit + CO_2). X = early mineral, I = late mineral.

formed by reactions that occurred during decompression after the peak of M3 metamorphism (discussed below). The decompression may have promoted fracturing of the garnet, allowing fluid access.

REACTIONS DURING UPLIFT AND COOLING

The Rauer boudins show a range of reaction textures that crosscut the D3 fabrics and which, therefore, probably postdate the peak of M3 metamorphism (Harley and Buick 1992; Buick et al. 1993). The reaction textures recognized in the boudins from Little Italy Island are summarized in Table 1 and include: (A) grandite replaced by wollastonite and scapolite symplectites; (B) grandite replaced by anorthite, wollastonite, and clinopyroxene; (C) scapolite replaced by wollastonite and plagioclase; (D) scapolite replaced by fine-grained anorthite and calcite; (E) fine-grained wollastonite rimming calcite; and (F) grossular rims on scapolite and wollastonite in the symplectites. The oxides also show some reaction textures, including: (G) rutile surrounded by ilmenite; and (H) titanite rimming ilmenite adjacent to calcite and quartz.

Because strong evidence exists from mineral textures in calcsilicate, metapelitic, and orthogneisses that the

FIGURE 3. Cathodoluminescence photomicrograph showing plagioclase (grey) and wollastonite (white) symplectite after scapolite, and garnet (black) cut by wollastonite filled fractures (width of view ~0.7 mm).

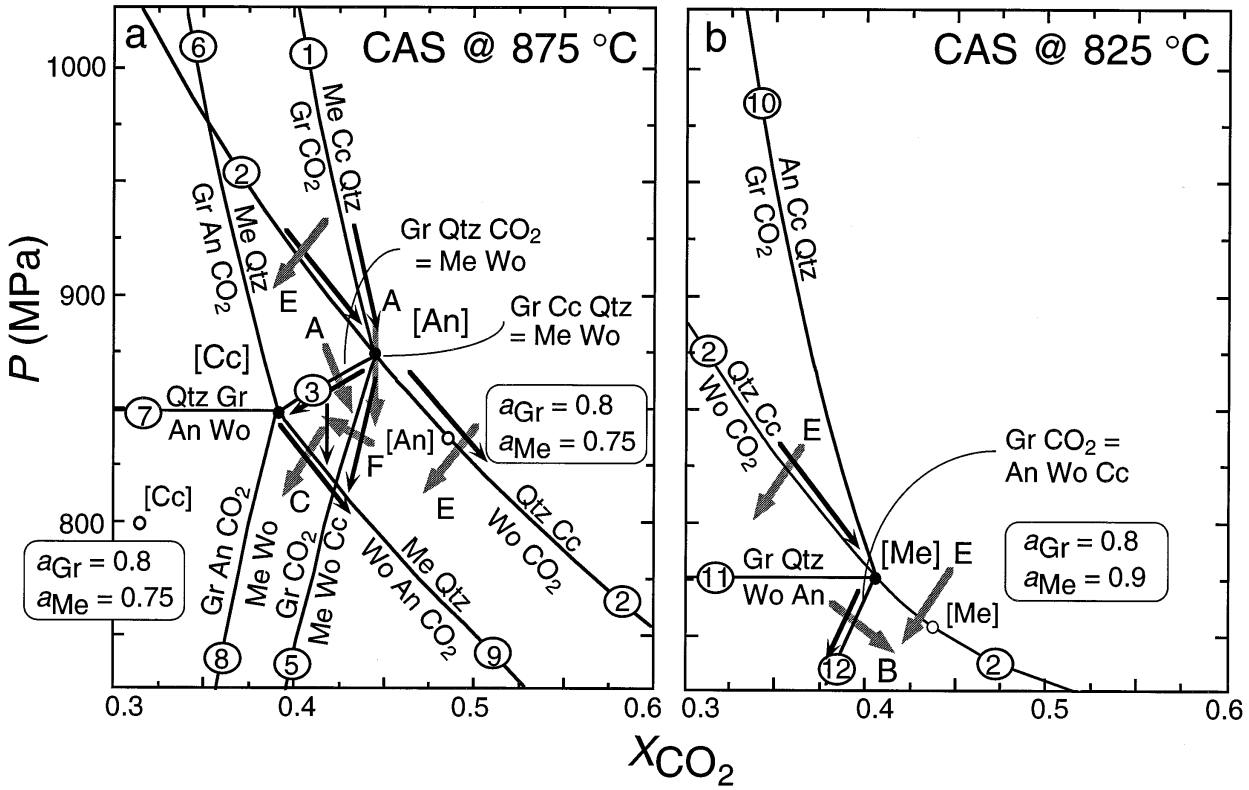

FIGURE 4. Isothermal P-X_{CO_2} diagrams at 875 and 825 °C showing reactions between anorthite, calcite, grossular, meionite, quartz, and wollastonite for fluid-present assemblages in the system CaO-Al_2O_3-SiO_2-CO_2-H_2O (CAS). The shaded lines in Figure 4 show the implied directions that the reactions were crossed from the textures discussed in the text (letters refer to textures outlined in Table 1), and the solid lines show possible buffering paths followed during decompression.

Prydz Bay rocks underwent near-isothermal decompression following the peak of M3 metamorphism (Harley 1988; Thost et al. 1991; Harley and Fitzsimons 1991; Harley and Buick 1992; Buick et al. 1993; Fitzsimons 1997), we will discuss the retrograde evolution of the boudins along a decompressional P-T path. Figure 4 shows reactions between anorthite, calcite, grossular, meionite, quartz, and wollastonite for fluid-present assemblages in the system CaO-Al_2O_3-SiO_2-CO_2-H_2O (CAS) in P-X_{CO_2} space at 875 and 825 °C, calculated using updated versions of the computer program Thermocalc (Powell and Holland 1989) and the Holland and Powell (1990) thermodynamic database (Powell, personal communication 1995). The geometry of the reactions in Figure 4a is generally valid at higher temperatures, whereas that in Figure 4b is appropriate at lower temperatures or for rocks with more meionite-rich scapolites. Typical activities reported by Harley and Buick (1992) for minerals from the boudins are: a_{Gr} = 0.8, a_{Me} = 0.75–0.9, a_{An} = 0.95–1.0, with calcite, quartz, and wollastonite being close to end-member compositions. The position of the reactions in Figure 4 have not been corrected for the compositions of the minerals in the calc-silicate boudins, as such activity-corrected phase diagrams that do not incorporate: (1) variations in mineral compositions along reaction lines that result from cation exchange reactions; or (2) the increase in variance of assemblages when additional components are present, are not strictly thermodynamically valid. Although quantitative pseudosections are probably the best way of depicting mineral reactions, in these rocks where mineral compositions are close to those in the end-member system, end-member P-X_{CO_2} diagrams provide a good guide to the reactions that may have affected the rocks.

We interpret the reaction textures as follows. The formation of wollastonite and scapolite symplectites (A) was by the fluid-absent reaction Gr + Cc + Qtz = Wo + Me, which occurs at the isothermal-invariant point [An], or by the fluid-present reaction Gr + Qtz + CO_2 = Wo + Me (3). The wollastonite microveins (Fig. 3), which presumably involved a fluid, may have been formed by the latter reaction. Formation of wollastonite + anorthite at the expense of scapolite + quartz (C) occurred by Me + Qtz = Wo + An + CO_2 (9). The replacement of calcite by wollastonite (E) was by the reaction Cc + Qtz = Wo + CO_2 (2), and the later grossular rims (F) were formed by the reaction Me + Wo + Cc = Gr + CO_2 (5). The formation of anorthite, wollastonite, and calcite at the expense of grandite (B) was by either the reaction Gr + CO_2 = An + Wo + Cc (12) or Gr + Qtz = Wo + An

(11). These reactions are not stable in Figure 4a but are in Figure 4b. The shaded lines in Figure 4 show the implied directions that the reactions were crossed. Most of these textures (with the exception of F) can be explained by down-pressure paths on P-X_{CO_2} diagrams, which is consistent with the reactions occurring during decompression from the peak of M3 metamorphism. The formation of fine-grained calcite and plagioclase at the expense of scapolite (D) was probably by the reaction Me = Cc + An, which may have been intersected during cooling following decompression (Harley and Buick 1992). The solid lines in Figure 4 show buffering paths that the zones in the boudins may have followed during decompression, with different zones possibly following different buffering paths.

Finite progress of fluid-present reactions occurred during decompression, implying that a fluid was present at that stage (e.g., Ferry 1994); however, the presence of internally buffered assemblages probably militates against the infiltration of large volumes of fluid. As discussed below, the pelites surrounding the boudins probably contained small volumes of a CO_2-bearing fluid while the reactions occurred. Minor infiltration or diffusion of that fluid into the boudins possibly initiated the fluid-present reactions. In detail, the pattern of fluid-rock interaction in the boudins may have been complicated. Some reactions, such as (9) and (2), produce fluids during decompression, and would help maintain any grain boundary fluid-filled porosity. By contrast, other reactions such as (3) and (12), would have consumed fluid. The fluids generated by the fluid-producing reactions may have aided the progress of the ones that consumed fluids.

While mineral activities cannot be used to calculate thermodynamically valid phase diagrams, they may be used to calculate X_{CO_2} values at given pressures and temperatures. Many of the possible buffering paths in Figure 4a pass through the [An] and [Cc] isothermally invariant points, while those in Figure 4b pass through the [Me] isothermally invariant point. The displaced positions of [An] and [Cc] for $a_{Gr} = 0.8$ and $a_{Me} = 0.75$ (with unit activities for all other minerals) at 875°C are ~830 MPa and $X_{CO_2} = 0.48$ and ~800 MPa and $X_{CO_2} = 0.33$, respectively. The displaced position of [Me] at 825 °C for $a_{Me} = 0.75$ and $a_{Gr} = 0.8$ is ~760 MPa and $X_{CO_2} = 0.43$. Overall, these data suggest that reactions occurred at 850–750 MPa in the presence of a fluid of $X_{CO_2} \approx 0.4$.

The minerals in the calc-silicate boudins contain small amounts of non-CAS components, notably Fe and Mg. The addition of Fe and Mg broadens the isothermally univariant reactions into fields. Additionally, as suggested by some of the reaction textures, the actual reactions involving garnet would have also involved clinopyroxene. However, the general form of the P-X_{CO_2} buffering paths in the extended system is similar to that discussed above (Harley and Buick 1992).

Titanite rimming ilmenite adjacent to calcite and quartz may have formed by a reaction in the CaO-FeO-TiO_2-SiO_2-CO_2 system: Qtz + Ilm + Cc = Fs + Tit + CO_2. In P-X_{CO_2} space, titanite is on the low-pressure side of this reaction, hence this mineralogic change probably also occurred during decompression.

Stable isotope geochemistry

Analytical techniques

Samples for stable isotope analysis were taken from ~50 × 20 × 5 mm blocks oriented parallel to the layering in the boudins. The blocks were cut into 7–9 pieces parallel to the layering and powdered for isotopic analysis. Stable isotope ratios were measured at Monash University. Oxygen isotope ratios of silicates from splits of the powder that had been treated with dilute HCl to remove calcite were analyzed following Clayton and Mayeda (1963) using ClF_3 as the oxidizing reagent. CO_2 was extracted from calcite by reaction with H_3PO_4 in sealed vessels at 25 °C for 2–4 h (McCrea 1950), the short reaction times minimizing the contribution of CO_2 from scapolite. CO_2 in scapolite was extracted by first reacting samples in H_3PO_4 at room temperature for 2–3 hours, while continually pumping to vacuum (to remove calcite), then continuing the reaction at 50–80 °C for 48–72 h. Graphite was reacted with CuO at 1000 °C to produce CO_2. Extracted gases were analyzed on a Finnigan MAT 252 mass spectrometer, and the results are expressed relative to V-PDB (C) and V-SMOW (O). Internal and international standards analyzed at the same time as the samples in this study generally yielded values within ±0.2‰ of their accepted values. Long term average of NBS 28 at Monash is 9.55 ± 0.11‰.

Carbon isotopes

The C isotope ratios from the boudins show the following features: (1) the three largest boudins (SH92-22, SH92-25, and SH92-26) show a fairly regular increase in $\delta^{13}C$(Cc) values from core to rim (Table 2, Fig. 5); (2) the boudin rims and the orthogneisses have closely similar $\delta^{13}C$(Cc) values of −10 to −9‰; and (3) the variation in core $\delta^{13}C$(Cc) values is >7‰, which is similar to the range reported by Buick et al. (1993) for boudins from different localities. Values of $\delta^{13}C$(Scp) vary sympathetically with $\delta^{13}C$(Cc). Average $\Delta^{13}C$(Cc-Scp) values from the boudins in this study are 0.56 ± 0.38‰ (Table 2). The predicted fractionation of ^{13}C between calcite and scapolite at granulite-facies conditions is ~0 to 2‰ (Moecher et al. 1994; Cartwright and Buick, unpublished data). While some scatter exists in the data, we conclude that the scapolite and calcite are in approximate isotopic equilibrium. Some scatter may reflect small-scale isotopic heterogeneities or analytical errors resulting from the two-stage dissolution process not completely removing the calcite. Graphite flakes in the pelite at the margin of boudin SH92-25 have $\delta^{13}C$ values of −18.5 to −20.4‰ (Table 2), which are somewhat lower than predicted for equilibrium with calcite at the margin of the boudin. As discussed below, the graphite may have been formed from fluid escaping from the boudin as a whole.

TABLE 2. Stable isotope ratios of calc-silicate boudins from Little Italy Island

Sample	Distance*	Cc (%)	Calcite		Silicate**		Scapolite	
			$\delta^{13}C$	$\delta^{18}O$	$\delta^{18}O$	$\Delta^{18}O$†	$\delta^{13}C$	$\Delta^{13}C$††
SH92-22R-a	8.44	4.9	−9.7	11.7				
SH92-22R-b	7.85	4.7	−10.3	12.1				
SH92-22R-c	7.26	5.8	−10.8	11.3				
SH92-22R-d	6.67	4.2	−10.6	11.7				
SH92-22R-e	6.08	1.3	−10.2	12.0				
SH92-22R-f	5.49	4.6	−12.7	12.5				
SH92-22R-g	4.90	1.0	−14.7	12.3				
SH92-22R-h	4.31	5.4	−15.6	12.7				
SH92-22C-a	3.72	3.5	−15.0	13.4			−15.5	0.5
SH92-22C-b	3.10	8.1	−16.1	11.9			−16.8	0.7
SH92-22C-c	2.48	8.3	−16.4	11.8				
SH92-22C-d	1.86	1.8	−16.4	12.9				
SH92-22C-e	1.24	4.6	−16.0	12.9			−17.0	1.0
SH92-22C-f	0.62	10.4	−17.3	12.3			−17.7	0.4
SH92-22C-g	0.00	12.2	−17.4	12.4			−18.6	1.2
SH92-25RD§	13.50				10.0			
SH92-25RC§	13.00		(−20.3)‖		10.8			
SH92-25RB§	12.50		(−19.2)‖		9.5			
SH92-25RA§	12.00		(−18.5)‖		10.4			
SH92-25I-a	9.52	0.8	−9.7	10.9	10.9	0.0		
SH92-25I-b	8.94	1.2	−9.6	11.4	11.4	0.0		
SH92-25I-c	8.36	2.7	−9.6	11.5	10.2	1.3		
SH92-25I-d	7.78	4.9	−10.4	11.5	10.5	1.0		
SH92-25I-e	7.20	5.8	−11.6	12.2	9.9	2.3		
SJ92-25I-f	6.62	5.2	−12.9	12.7	11.5	1.2		
SH92-25I-g	6.04	4.3	−15.3	12.2	10.6	1.6		
SH92-25I-h	5.46	5.0	−16.4	13.5	11.0	2.5		
SH92-25C-i	4.88	3.9	−16.1	13.6	10.4	3.2		
SH92-25C-h	4.27	5.1	−15.6	12.3	10.4	1.9		
SH92-25C-g	3.66	4.4	−15.9	14.1	10.0	4.1		
SH92-25C-f	3.05	3.9	−15.6	13.0	10.7	2.3		
SH92-25C-e	2.44	1.7	−16.7	12.2	10.4	1.8		
SH92-25C-c	1.22	5.6	−17.5	13.1	10.1	3.0		
SH92-25C-b	0.61	3.0	−17.0	13.5	10.5	3.0		
SH92-25C-a	0.00	2.9	−16.2	13.4	11.4	2.0		
SH92-26R2-a	9.04	1.6	−9.3	11.7	9.2	2.5		
SH92-26R2-b	8.49	1.2	−9.1	11.9				
SH92-26R2-c	7.94	1.0	−10.6	12.5	9.4	3.1		
SH92-26R2-d	7.39	2.0	−10.8	12.2				
SH92-26R2-e	6.84	1.9	−11.6	12.2				
SH92-26R2-f	6.29	2.7	−11.6	12.5	9.5	3.0		
SH92-26R2-g	5.74	3.9	−11.7	12.2				
SH92-26R2-h	5.19	4.1	−11.9	12.2				
SH92-26C-a	4.64	1.5	−11.8	14.6				
SH92-26C-b	4.06	3.1	−11.8	13.2				
SH92-26C-c	3.48	1.8	−11.6	13.3	10.1	3.2		
SH92-26C-d	2.90	1.6	−11.7	14.2	10.3	3.9		
SH92-26C-e	2.32	1.5	−11.9	12.8			−12.8	0.9
SH92-26C-f	1.74	1.4	−12.5	14.8	10.4	4.4	−12.4	−0.1
SH92-26C-g	1.16	1.0	−13.6	14.2				
SH92-26C-h	0.58	1.8	−13.0	14.8				
SH92-26C-i	0.00	1.4	−12.6	14.1	11.1	3.0	−13.0	0.4
SH92-29a	5.52	1.3	−8.9	11.5	9.4	2.1		
SH92-29b	4.83	6.0	−9.2	11.7				
SH92-29c	4.14	8.1	−10.6	11.0	9.3	1.7		
SH92-29d	3.45	8.9	−9.6	12.0				
SH92-29e	2.76	7.9	−9.3	11.7				
SH92-29f	2.07	7.6	−9.5	12.1	10.0	2.1		
SH92-29g	1.38	6.9	−9.7	12.4				
SH92-29h	0.69	2.7	−9.7	12.7	10.2	2.5		
SH92-29i	0.00	3.4	−9.9	13.7	9.7	4.0		
SH92-30E-a	4.69	2.4	−9.2	12.6	9.6	3.0		
SH92-30E-b	4.02	6.6	−9.8	11.5				
SH92-30E-c	3.35	7.1	−10.5	11.3			−10.8	0.3
SH92-30E-d	2.68	4.9	−10.3	11.6	9.4	2.2		
SH92-30E-e	2.01	6.1	−10.3	12.3			−10.5	0.2
SH92-30E-f	1.34	5.0	−9.9	11.7	9.5	2.2	−10.6	0.7
SH92-30E-g	0.67	8.5	−10.3	11.6				
SH92-30E-h	0.00	4.1	−10.0	12.7	11.9	0.8		
SH92-30W-a	4.26	3.1	−10.2	12.5	9.6	2.9		
SH92-30W-b	3.55	2.9	−10.0	12.5	9.4	3.1		
SH92-30W-c	2.84	2.9	−9.8	12.8	9.4	3.4		

TABLE 2—*Continued*

Sample	Distance*	Cc (%)	Calcite		Silicate**		Scapolite	
			$\delta^{13}C$	$\delta^{18}O$	$\delta^{18}O$	$\Delta^{18}O$†	$\delta^{13}C$	$\Delta^{13}C$††
SH92-30W-d	2.13	3.5	−9.8	13.2	9.2	4.0		
SH92-30W-e	1.42	6.3	−9.7	11.8	9.5	2.3		
SH92-30W-f	0.71	8.5	−11.1	11.2	9.5	1.7		
SH92-30W-g	0.00	7.9	−10.7	11.2	9.6	1.6		
Average					10.13	2.41		0.56
σ					0.72	1.05		0.38

* Distance from centre of boudin.
** $\delta^{18}O$ of bulk silicate fraction.
† $\delta^{18}O(Cc) - \delta^{18}O(Silicate)$.
†† $\delta^{13}C(Cc) - \delta^{13}C(Scap)$.
§ Paragneiss adjacent to boudin.
‖ $\delta^{13}C$(Graphite).

The boudins probably underwent a period of fluid infiltration before the peak of M3 metamorphism that stabilized the wollastonite-bearing assemblages (Harley and Buick 1992). Decarbonation during this fluid infiltration episode would have probably produced both the low calcite contents and the low $\delta^{13}C(Cc)$ values recorded from the boudin cores. However, as discussed below, the distinct $\delta^{13}C(Cc)$ core-rim trends in the boudins are unlikely to have formed during this early fluid infiltration episode, but were most probably formed by diffusion during uplift and cooling from the peak of M3 metamorphism following the bondinage of the calc-silicate layers.

Oxygen isotopes

The $\delta^{18}O(Cc)$ values vary much less than the $\delta^{13}C(Cc)$ values, although boudins SH92-25, SH92-26, and SH92-29 show slight decreases in $\delta^{18}O(Cc)$ values from core to rim. The $\delta^{18}O$ values of the bulk silicate fraction also show little variation from the boudin core to rim. The average $\delta^{18}O(Silicate)$ value (10.1 ± 0.7‰) is within the range of the $\delta^{18}O$ values from the gneisses surrounding boudin SH92-25 (9.5–10.8‰). The early infiltration of water-rich fluids from the surrounding gneisses would have probably homogenized the $\delta^{18}O$ values. The difference between $\delta^{18}O(Cc)$ and $\delta^{18}O(Silicate)$ values from the same sample of boudin are somewhat variable (0.0–4.4‰, average 2.4 ± 1.0‰), which may be due to the small-scale variation in mineralogy within the boudins. Closed-system resetting of oxygen isotopes during cooling from the peak of M3 metamorphism will potentially result in variable $\delta^{18}O(Cc)$ values if the calcite in different domains coexists with variable amounts of minerals (e.g., garnet, clinopyroxene, wollastonite, and scapolite) that have contrasting $^{18}O/^{16}O$ fractionations.

DISCUSSION

We interpret the $\delta^{13}C$ profiles in Figure 5 as forming by isotopic exchange between the boudins and the surrounding gneisses. The timing, duration, and processes of isotopic exchange and the nature of the carbon reservoir in the gneisses are discussed below.

Timing of formation of carbon isotope profiles

As discussed above, the calc-silicate rocks that form the boudins were probably infiltrated by fluids prior to the peak of M3 metamorphism in an event that stabilized wollastonite-bearing assemblages in the boudin cores and lowered $\delta^{13}C$ values. However, because the $\delta^{13}C$ profiles are developed between the cores and rims of the boudins, the shape of which was produced by later deformation at the peak of M3 metamorphism, the profiles were probably formed at or after the M3 peak. In addition, the development of the carbon isotope profiles probably occurred at the same time as the formation of the graphite in the pelites. The graphite crosscuts the D3 fabrics, suggesting that it formed after the peak of M3 metamorphism.

Rates of isotopic diffusion within minerals are probably several orders of magnitude slower than those in fluids (e.g., Cole and Ohmoto 1986), and it is commonly assumed that centimeter-scale isotopic transport requires the presence of a fluid phase. However, at high temperatures, isotopic transport along grain boundaries may be relatively rapid regardless of whether or not a fluid phase is present (Farver and Yund 1991), and centimeter-scale $\delta^{18}O$ profiles in granulites have been interpreted as forming by diffusion under anhydrous conditions (Todd and Evans 1993). Therefore, the carbon isotope profiles could reflect diffusion close to the peak of M3 metamorphism, after the D3 deformation (which is the time that Buick et al. 1993 suggested that diffusion formed the geochemical zonation). While recognizing this possibility, we consider that it is more likely that the resetting of carbon isotopes occurred during the period when the late reaction textures formed. As discussed above, progress of the isothermally univariant reactions to form the late symplectites requires the presence of a fluid phase, and some of the reactions intersected during decompression would have produced a fluid. Fluid production could have resulted in a reaction-enhanced porosity-permeability (c.f. Rumble and Spear 1983) that would have facilitated isotopic exchange. In addition to the role that the reactions may have had in producing fluids and enhancing the porosity and permeability, small-scale isotopic exchange between individual

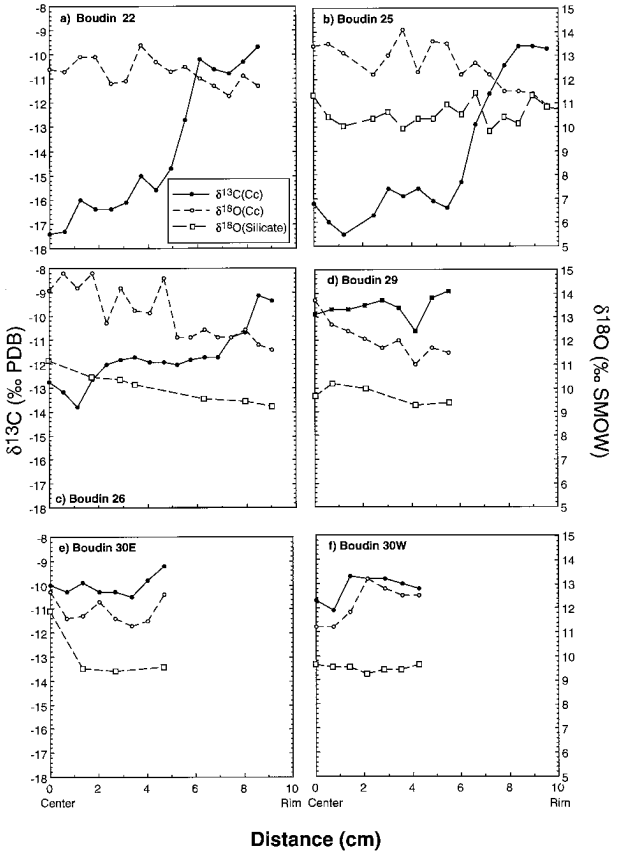

FIGURE 5. Carbon and oxygen isotope profiles across the Little Italy boudins. $\delta^{13}C(Cc)$ values increase irregularly from core (as low as −18 to −17‰) to rim (−10 to −9‰). As discussed in the text such changes probably reflect fluid-hosted diffusion during decompression from the M3 metamorphic peak. $\delta^{18}O$ values of calcite and silicate fractions do not show such regular variation, possible due to homogenization by fluid flow prior to the peak of M3 metamorphism.

grains and the fluid would probably have been facilitated by recrystallization reducing effective grain sizes. In the absence of recrystallization, significant isotopic transport through the minerals may not be possible, limiting the degree of isotopic exchange regardless of the rate of grain-boundary transport. Steep $\delta^{18}O$ profiles recorded from within grains by Eiler et al. (1995) attest to the sluggishness of intracrystalline isotopic diffusion even at high temperatures. Steep oxygen isotope profiles of several per mil over a few centimeters between anhydrous granulite-facies gneisses in other terrains (e.g., Cartwright and Valley 1992) also imply limited exchange. In addition, Sharp et al. (1988) show a correlation between recrystallization and isotopic exchange in ironstones deformed under amphibolite-facies conditions from Wind River (USA). Likewise, syenitic orthogneisses from the Adirondack Mountains (USA) that underwent shearing at greenschist to lower amphibolite facies grades under fluid-present conditions show a correlation between the intensity of recrystallization and the completeness of isotopic exchange with the fluid (Cartwright et al. 1993). Thus, we suggest that the combination of recrystallization and the presence of a fluid was required for isotopic exchange to occur.

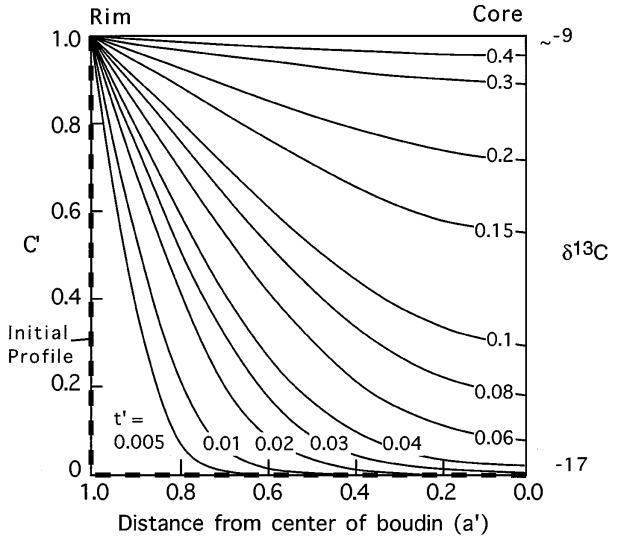

FIGURE 6. Geochemical profiles resulting from spherical diffusion at different dimensionless times, $t' = (D_e t K_e^{-1})/a^2$, where D_e is the effective diffusion coefficient, t is time, K_e is the rock-fluid partition coefficient and a is boudin radius. The profiles in Figure 5 resemble those predicted for spherical diffusion.

Diffusion of C isotopes

The $\delta^{13}C(Cc)$ profiles from boudins SH92-22, SH92-25, and SH92-26 are similar to those predicted to result from diffusion of a tracer within a sphere that is surrounded by a well-mixed, homogeneous, infinite reservoir (e.g. Crank 1975). As a first approximation, the boudin profiles may be analyzed using that model. We initially make the following assumptions that are based on the data presented above: (1) prior to diffusion the whole boudin had a $\delta^{13}C(Cc)$ of −17‰; (2) the surrounding paragneiss contained a carbon reservoir that is in equilibrium with calcite of $\delta^{13}C = -9$‰ (the nature of this reservoir is discussed below); (3) the boudin had a uniform calcite content of 5 wt%; and (4) diffusion was uniform in all directions. Figure 6 shows the general form of geochemical profiles resulting from spherical diffusion. The curves in Figure 6 are labelled in terms of dimensionless time t' ($t' = (D_e t K_e^{-1})/a^2$), where D_e is the effective diffusion coefficient, t is time, K_e is the rock-fluid partition coefficient and a is the boudin radius. For small porosities, K_e is given by:

$$K_e \approx \frac{\rho_s \cdot K_c}{\rho_f}$$

where K_c is the relative amount of C in the rock and the fluid and ρ_s and ρ_f are the densities of the fluid and solid (e.g. Bickle and Baker 1990). As discussed earlier, fluids in the boudins had X_{CO_2} values of ~0.4, which equates to

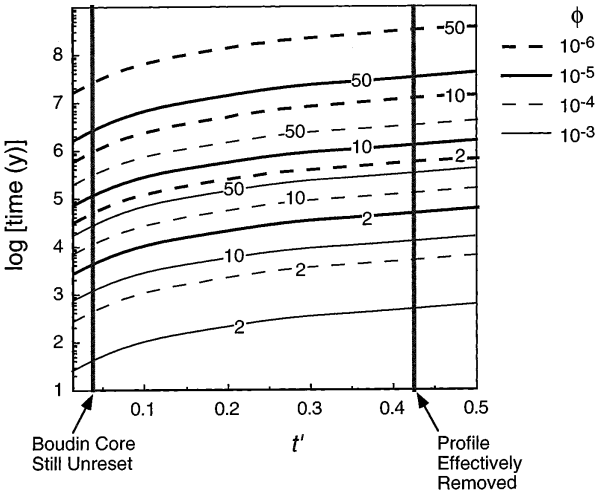

FIGURE 7. Time required to form the observed $\delta^{13}C$ profiles for a range of porosities and boudin radii (labelled curves) calculated using Figure 6. Unless porosities were very small (10^{-6}–10^{-5}) preservation of the $\delta^{13}C$ profiles implies that diffusion only occurred over <1 Ma.

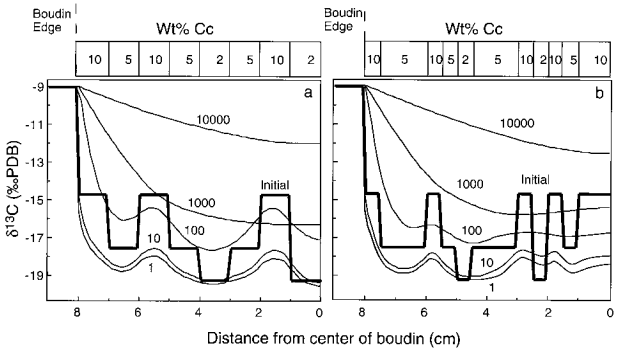

FIGURE 8. Evolution of $\delta^{13}C$ profiles in an 8 cm radii boudins that initially contains eight layers of slightly different calcite contents (2 to 10 wt%) modeled using Fractran (Sudicky and McLaren 1992). Across the model boudin, there is a correlated initial variation in wt% calcite and $\delta^{13}C$ values (from −19 to −15‰). Diffusion proceeds such that the small-wavelength variations are homogenized over much shorter time scales (a few years) than the profile as a whole.

17 wt% C in the fluid. If the rock contained 5 wt% calcite it had a total C content of 0.6 wt%. For these calcite contents, a rock density of 2700 kg/m^3 and a fluid density of ~950 kg/m^3 (Brown and Lamb 1989), K_e values for C are ~0.1. A diffusion coefficient for C in fluid (D_f) of 10^{-8} m^2/sec was used, which is similar to the diffusion coefficients for O in metamorphic fluids (Bickle and McKenzie 1987).

As discussed above, we interpret the centimeter-scale diffusion as being via a grain-boundary fluid. Since fluid-hosted diffusion is relatively rapid compared with diffusion within minerals, we will assume that $D_e \approx D_f\phi$, where ϕ is the porosity. Figure 7 shows the time taken to form the profiles for a range of porosities and boudin radii. If boudins SH92-22 and SH92-25, which have radii of ~10 cm, are preserving unaltered core compositions, t' as estimated from Figure 6 is ~0.03. For metamorphic porosities of 10^{-3}, the time taken to form such a profile in a 10 cm radius boudin is only $\sim 1 \times 10^3$y; while for lower porosities of 10^{-5}–10^{-4} the time required to form the profiles (assuming $t' = 0.03$) increases to 10–100 $\times$ 10^3y (Fig. 7). The cores of these boudins may have been reset, in which case t' values would be slightly higher. However, the lowest $\delta^{13}C$(Cc) values recorded from Rauer Group boudin cores are ~−21‰ (Buick et al. 1993). Given that it is difficult to produce much lower $\delta^{13}C$ values by decarbonation in calc-silicate rocks like these that do not contain graphite, it is hard to conceive that the boudin cores initially had much lower $\delta^{13}C$ values. Even if the cores of these boudins were raised by 2–3‰ during diffusion, t' values would still be <0.1 which does not drastically alter the time estimates. If boudin 92SH-26 (radius ~9 cm) initially had a $\delta^{13}C$(Cc) value of −17‰, t' values would be ~0.15. In this case it would take ~8–800 ka to produce the profile if porosities were in the range 10^{-5} to 10^{-3}. Boudins 92SH-29, 92SH-30E, and 92SH-30W show little in the way of isotopic zonation. Again assuming that these boudins initially had much lower $\delta^{13}C$ values, t' may be around 0.4–0.5. These boudins are smaller (~5 cm radius), which may account for their more reset profiles. Some boudins contain slightly more or less calcite than others; however, the calculations are not significantly affected by this or by slight variations in fluid composition.

Except for very large boudins or very low porosities, the preservation of the isotopic profiles requires diffusion to have operated only for relatively short time spans (<1 Ma). The timescales are much shorter than those estimated for the duration of uplift (~15 Ma) and may reflect the time over which the metamorphic reactions occurred and a fluid phase was present. If this was the case, porosities may have been closer to the higher estimates in Figure 7, implying that diffusion took place over only a few thousand years. Diffusion may have ceased when the fluid escaped from the rocks, which would have caused the fluid-present reactions to cease and retard the rate of isotopic transport along the grain boundaries. Fluid escape may have been due to hydrofracturing of the rock caused by an expansion of the fluid during decompression.

Initial variations in $\delta^{13}C$

The models above assume that the boudins had uniform $\delta^{13}C$ values prior to diffusion, and that K_e values were constant. However, if these boudins represent skarns that originally formed by fluid infiltration and decarbonation prior to granulite-facies metamorphism, they may have had heterogeneous $\delta^{13}C$ values prior to the diffusion episode. In addition, calcite contents vary by a few wt% within individual boudins. We will therefore extend the modeling using the numerical model Fractran (Sudicky and McLaren 1992) which can simulate tracer diffusion in porous media. Figure 8a shows the evolution of $\delta^{13}C$

profiles in an 8 cm radius boudin which initially contains 8 layers of slightly different calcite contents (2 to 10 wt%). We have assumed that $\delta^{13}C$ values and wt% calcite were initially correlated as is expected in rocks where variable decarbonation has occurred (Valley 1986; Nabelek 1991). Hence, across the model boudin, there is a correlated initial variation in wt% calcite and $\delta^{13}C$ values (from −19 to −15‰). We have modeled the boudin as a body of finite width within a large reservoir (the gneisses) that has uniform $\delta^{13}C$ values (−9‰). K_e values calculated for the individual zones as outlined above, and assuming a fluid of $X_{CO_2} = 0.4$, vary from 0.2 to 0.05. D_e was taken as 10^{-11} m²/sec.

Diffusion within the model proceeds such that the small-wavelength variations are homogenized over much shorter time scales (a few years) than the profile as a whole. Figure 8b shows a similar model, but this time with internal layers that vary from 0.5 to 1.5 cm in width. Here the smaller initial $\delta^{13}C$ fluctuations are homogenized even faster than the fluctuations in Figure 8a. These findings are to be expected as the time required for diffusion to remove an initial discontinuity is inversely proportional to the square of the width of the diffusion domain (Crank 1975). These models are one-dimensional; however, they serve to illustrate that small scale fluctuations in $\delta^{13}C$ values would have been probably removed on a smaller time scale than homogenization of $\delta^{13}C$ values across the boudin. The $\delta^{13}C$ profiles as a whole in Figure 8 are reset over similar time scales to those predicted using the simple spherical diffusion model. The irregularities in the $\delta^{13}C$ profiles in Figure 5 may reflect initial variations that were not completely removed before the fluid escaped from the rock.

Origin of CO_2-bearing fluids in the metapelites

If the profiles discussed above were produced by diffusion, the pelites must have contained a reservoir of carbon. The similarity of $\delta^{13}C$(Cc) values at the boudin rims implies that this carbon reservoir had reasonably uniform $\delta^{13}C$ values. Except immediately adjacent to the boudins, the pelites do not contain graphite, calcite, or scapolite, suggesting that the C was hosted in a C-O-H fluid. Calcite at the margins of the boudins has $\delta^{13}C$ values of −10 to −9‰. At 800°C $\Delta^{13}C(CO_2\text{-Cc})$ values are ~−3‰ (Chacko et al. 1991), implying that the fluid would have had a $\delta^{13}C$ value of ~−7 to −6‰. These values are much higher than those typical of Archaean graphite and fall within the range of igneous or mantle values (Hoefs 1987). It is possible that the CO_2 was introduced into the pelites during the granulite-facies metamorphism by a mantle-derived fluid (c.f. Newton et al. 1980); however, widespread infiltration of large volumes of CO_2 is unlikely because of: (1) the absence of replacement of pyroxene-plagioclase assemblages in the metabasites by scapolite (Harley 1987); and (2) some partial melting of the metasediments occurred during M3. There are several other possible origins for this CO_2-bearing fluid. The fluid may have been the residual fluid after anatexis had partitioned water from any initially mixed-volatile fluid into the melts. At 840°C and 700–900 MPa, fluids in equilibrium with granitic melts are expected to have X_{CO_2} values of 0.6–0.8 (Newton 1986). Marbles in the Rauer group underwent pre-M3 fluid infiltration and have $\delta^{13}C$ values as low as −7‰ (Buick et al. 1994); it is possible that small amounts of fluids from these marbles infiltrated the pelites during M3. Alternatively, there was extensive emplacement of dioritic to granitic orthogneisses late in M3 which may have contained minor volumes of CO_2. The crystallization of these rocks may also have liberated fluids. The crystallization of partial melts that were formed during M3 metamorphism are another potential fluid source, and fluids from these melts may have caused the incipient retrogression in the pelitic gneisses. However, the temperatures at which the reactions are inferred to have occurred are somewhat higher that the temperatures at which crystallizing partial melts exsolve fluids (~650 °C; e.g. Cartwright 1988). Whatever the source, minor infiltration or diffusion of this fluid into the boudins probably promoted the metamorphic reactions.

Graphite formation

The outer zones of some of the boudins contain a small amount (<1%) of texturally-late graphite. As the boudins and the paragneisses in this area are generally graphite free, the presence of this graphite is probably related to processes occurring in the boudins. The infiltration of CO_2-rich fluids into reduced granulite-facies rocks is likely to stabilize graphite (Lamb and Valley 1984), and the presence of graphite in the Rauer rocks may be related to variations in f_{O_2} around the boudins. Ilmenite in the almandine zone of 95SH-29 has a composition of XIlm = 0.948 (Cartwright, unpublished data). Magnetite in this sample has low Ti contents and is surrounded by small blebs of ilmenite that are probably the result of exsolution during cooling. Unfortunately, none of the magnetites display the types of trellis exsolution that are amenable to reintegration to determine the original magnetite composition (e.g., Bohlen and Essene 1977). However, if the ilmenite composition has not been reset during cooling, it is possible to use the temperature to estimate the initial magnetite composition and f_{O_2} (Cartwright et al. 1993). Figure 9 shows a f_{O_2} vs. temperature plot for the ilmenite-magnetite system at 700 MPa (data from Anderson and Lindsley 1988). As the graphite formed late, we chose a pressure at the low end of those implied by Figure 4. The mineral composition isopleths are plotted relative to the fayalite-magnetite-quartz (Fa-Mt-Qtz) buffer where $\Delta\log f_{O_2}$ (Fa-Mt-Qtz) is defined as $\log f_{O_2} - \log f_{O_{2(\text{Fa-Mt-Qtz})}}$ at the temperature of interest and 700 MPa. Values of $\log f_{O_{2(\text{Fa-Mt-Qtz})}}$ were again calculated using updated versions of Thermocalc and the Holland and Powell (1990) thermodynamic database. The composition of magnetite in equilibrium with ilmenite of $X_{Ilm} = 0.948$ is given by the intersection of the X_{Usp} isopleths with the $X_{Ilm} = 0.948$ isopleth. As discussed above, decompression probably occurred at 800–850 °C. At these temperatures the esti-

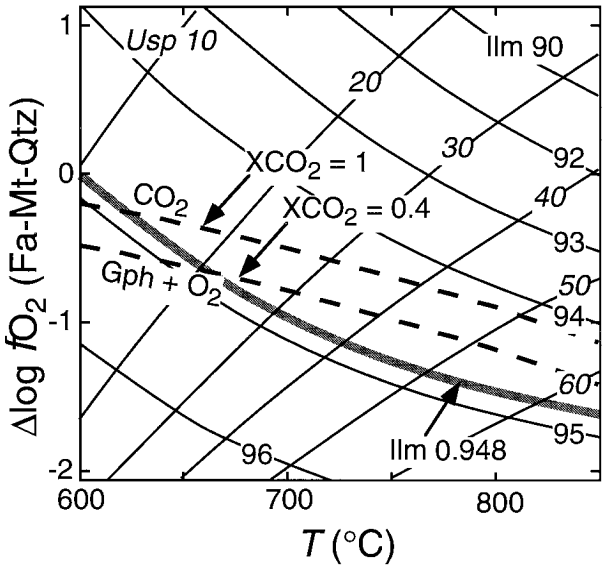

FIGURE 9. f_{O_2} vs. T plot for the ilmenite-magnetite system at 700 MPa (after Anderson and Lindsley 1988) with mineral composition isopleths plotted relative to the fayalite-magnetite-quartz (Fa-Mt-Qtz) buffer at the temperature of interest and 700 MPa. The composition of magnetite in equilibrium with ilmenite of $X_{Ilm} = 0.948$ at 800–850 °C is $X_{Usp} \approx 0.6$, which suggests f_{O_2} conditions within the graphite stability field (at $X_{CO_2} = 0.4$–1.0). Hence, the influx of a CO_2-bearing fluid from the boudin core could have resulted in the precipitation of graphite in the Almandine zone.

mated magnetite composition is $X_{Usp} \approx 0.6$ which suggests f_{O_2} conditions within the graphite stability field (at $X_{CO_2} = 0.4$–1.0). Hence, the influx of a CO_2-bearing fluid produced by the reactions in the boudin core could have resulted in graphite precipitating in the Almandine zone.

The graphite in the pelites around 92SH-25 has $\delta^{13}C$ values of −18.5 to −19.3‰. At 800 °C, the predicted fractionation of carbon isotopes between calcite and graphite is ~3.1‰ (Kitchen and Valley 1995). Calcite from the margin of this boudin has $\delta^{13}C$ values of −9.7‰, while calcite in the center has $\delta^{13}C$ values as low as −17.5‰. CO_2 in isotopic equilibrium with calcite in this boudin would be expected to precipitate graphite with $\delta^{13}C$ values of −20.6 to −12.8‰, which spans the measured values. As previously discussed, diffusion probably ceased when the fluid phase escaped from the rock. Just prior to escaping, the fluid would have had a range of $\delta^{13}C$ values similar to that observed in the boudin calcite, and it is possible that the graphite was precipitated from a fluid escaping from all zones of the boudin that has a ''mixed'' isotopic signature. If that was the case, the precipitation of graphite would have represented the last fluid-related event in these rocks.

Implications

The results of this study illustrate some of the complexities in understanding the timing and processes of isotopic exchange. We have proposed that carbon isotope exchange in the Rauer rocks was facilitated by the presence of fluids and recrystallization during retrogression. Whether recrystallization is required for significant isotopic exchange to occur could be assessed by comparison of the $\delta^{13}C$ profiles developed in these Rauer rocks with ones developed in similar lithologies that did not undergo reaction during uplift and cooling. Additionally, for the Rauer boudins, isotopic exchange required a source of carbon in the surrounding gneisses. If the carbon was present in a fluid, the timing of exchange would have been controlled by when that fluid was present.

ACKNOWLEDGMENTS

This research was supported by ARC grants A39030662 and A39231141 (to IC), and IC gratefully acknowledges receipt of an ARC Queen Elizabeth II Fellowship. ISB was supported by an ARC Australian Research Fellowship. We thank M. Jane and D. Korke for help with the stable isotope analyses, M. Wallace for the use of the cathodoluminescence equipment, and T. Weaver for explaining FRACTRAN. The paper was improved by reviews from P.I. Nabelek and C. Todd and editorial advice from J. Morrison.

REFERENCES CITED

Anderson, D.J., and Lindsley, D.H. (1988) Internally consistent solution models for Fe-Mg-Mn-Ti oxides: Fe-Ti oxides. American Mineralogist, 73, 714–726.

Bickle, M.J., and Baker, J. (1990) Advective-diffusive transport of isotopic fronts: an example from Naxos, Greece. Earth and Planetary Science Letters, 97, 79–93.

Bickle, M.J., and McKenzie, D. (1987) The transport of heat and matter by fluids during metamorphism. Contributions to Mineralogy and Petrology, 95, 384–392.

Bohlen, S.R., and Essene, E.J. (1977) Feldspar and oxide thermometry of granulites in the Adirondack Highlands. Contributions to Mineralogy and Petrology, 62, 153–169.

Brown, P.E., and Lamb, W.M. (1989) P-V-T properties of fluids in the system $H_2O \pm CO_2 \pm$ NaCl: New graphical presentations and implications for fluid inclusion studies, Geochimica et Cosmochimica Acta, 53, 1209–1221.

Buick, I.S., and Cartwright, I. (1995) Petrological and stable isotopic studies of early contact metamorphism of the Reynolds Range Group, central Australia: implications for the distribution of fluids during LP-HT metamorphism. Australian Journal of Earth Science, 42, 301–310.

———(1996) Channelled high-temperature retrogression of granulites from the Reynolds Range Group, central Australia. Journal of Petrology, in press.

Buick, I.S., Harley, S.L., and Cartwright, I. (1993) Granulite facies metasomatism: zoned calc-silicate boudins from the Rauer Group, East Antarctica. Contributions to Mineralogy and Petrology, 113, 557–571.

Buick, I.S., Cartwright, I., Hand, M., and Powell, R. (1994) Evidence for pre-regional metamorphic fluid infiltration of the Lower Calcsilicate Unit, Reynolds Range Group (central Australia). Journal of Metamorphic Geology, 12, 789–810.

Carson, C.J., Fanning, C.M., Wilson, C.J.L., and Powell, R. (1995) Early Palaeozoic evolution of southwest Prydz Bay, East Antarctica. Abstracts of the VII International Symposium on Antarctic Earth Sciences.

Cartwright, I. (1988) Melt crystallisation, pegmatite intrusion and the Inverian retrogression of the Scourian complex of NW Scotland. Journal of Metamorphic Geology, 6, 77–93.

Cartwright, I., and Buick, I.S. (1995) Formation of wollastonite-bearing marbles during late-regional metamorphic channelled fluid flow in the Upper Calc-silicate Unit, Reynolds Range Group, central Australia. Journal of Metamorphic Geology, 13, 397–418.

Cartwright, I., and Valley, J.W. (1991) Steep oxygen-isotope gradients at the contacts between metagranites and marbles in the northwestern Ad-

irondack Mountains, New York: Products of fluid-hosted diffusion. Earth and Planetary Science Letters, 107, 148–163.

———(1992) Oxygen-isotope geochemistry of the Scourian complex, NW Scotland. Journal of the Geological Society, London, 149, 115–126.

Cartwright, I., Valley, J.W., and Hazelwood, A.M. (1993) Extent and causes of resetting of oxybarometers and oxygen isotopes in granulite-facies orthogneisses: Diana and Stark complexes, NW Adirondack Mountains, New York. Contributions to Mineralogy and Petrology, 113, 208–225.

Chacko, T., Mayeda, T.K., Clayton, R.N., and Goldsmith, J.R. (1991) Oxygen and carbon fractionations between CO_2 and calcite. Geochimica et Cosmochimica Acta, 55, 2867–2882.

Clayton, R.N., and Mayeda, T.K. (1963) The use of bromine pentafluoride in the extraction of oxygen from oxides and silicates for isotopic analysis. Geochimica et Cosmochimica Acta, 27, 43–52.

Cole, D.R., and Ohmoto, H. (1986) Kinetics of isotopic exchange at elevated temperatures and pressures. In J.W. Valley, H.P. Taylor, and J.R. O'Neil, Eds., Stable Isotopes in High Temperature Geological Processes. Mineralogical Society of America Reviews in Mineralogy, 16, 41–90.

Corbett, G.J., and Phillips, G.N. (1981) Regional metamorphism of a high grade terrain: The Willyama complex, Broken Hill, Australia. Lithos, 14, 59–79.

Crank, J. (1975) The Mathematics of Diffusion, 414 p. Oxford University Press, Oxford, U.K.

Eiler, J.M., Valley, J.W., Graham, C.M., and Baumgartner, L.P. (1995) The oxygen isotope anatomy of a slowly cooled metamorphic rock. American Mineralogist, 80, 757–764.

Farver, J.R., and Yund, R.A. (1991) Measurement of oxygen grain boundary diffusion in natural fine-grained quartz aggregates. Geochimica et Cosmochimica Acta, 55, 1597–1608.

Ferry, J.M. (1994) Role of fluid flow in the contact metamorphism of siliceous dolomitic limestones. American Mineralogist, 79, 719–736.

Fitzsimons, I.C.W. (1996) The Brattstrand Paragneiss and the Søstrene Orthogneiss: A review of Pan-African metamorphism and Grenvillian relics in southern Prydz Bay. Proceedings of the VII International Symposium on Antarctic Earth Sciences. in press.

Harley, S.L. (1987) Precambrian geological relationships of the Rauer Islands, East Antarctica. Australian Journal of Earth Sciences, 34, 175–207.

———(1988) Proterozoic granulites from the Rauer Group, East Antarctica. I: Decompressional pressure-temperature paths deduced from mafic and felsic gneisses. Journal of Petrology, 29, 1059–1095.

Harley, S.L., and Buick, I.S. (1992) Wollastonite-Scapolite assemblages as indicators of granulite Pressure-Temperature-fluid histories: application to the Rauer Group, East Antarctica and other high grade terrains. Journal of Petrology, 33, 693–728.

Harley, S.L., and Fitzsimons, I.C.W. (1991) Pressure-temperature evolution of metapelitic granulites in a polymetamorphic terrane: The Rauer Group, East Antarctica. Journal of Metamorphic Geology, 9, 231–243.

———(1995) High grade metamorphism and deformation in the Prydz Bay region, East Antarctica: terranes, events and regional correlations. Journal of the Geological Society of India, 34, 73–100.

Harley, S.L., Fitzsimons, I.C.W., Buick, I.S., and Watt, G (1992) The significance of reworking, fluids and partial melting in granulite metamorphism, East Prydz Bay, Antarctica. In Y. Yoshida, K. Kaminuma, and K.Shiraishi, Eds. Recent Progress in Antarctic Earth Science, p. 119–127, Terra Scientific Publishing, Tokyo.

Harley, S.L., Snape, I., and Fitzsimons, I.C.W. (1995) Regional correlations and terrane assembly in East Prydz Bay: evidence from the Rauer Group and Vestfold Hills. Terra Antarctica, 2, 49–60.

Hensen, B.J. and Zhou, B. (1995) A Pan-African granulite facies metamorphic episode in Prydz Bay, Antarctica: Evidence from Sm-Nd garnet dating. Australian Journal of Earth Science, 42, 245–258.

Hoefs, J. (1987) Stable Isotope Geochemistry (3rd edition). 241 p. Springer-Verlag, Berlin.

Holland, T.J.B., and Powell, R (1990) An enlarged and updated internally consistent thermodynamic dataset with uncertainties and correlations: The system K_2O-Na_2O-CaO-MgO-MnO-FeO-Fe_2O_3-Al_2O_3-TiO_2-SiO_2-C-H_2-O_2. Journal of Metamorphic Geology, 8, 89–124.

Kinny, P.D., Black, L.P., and Sheraton, J.W. (1993) Zircon ages and the distribution of Archaean and Proterozoic rocks in the Rauer Islands. Antarctic Science, 5, 193–206.

Kitchen, N.E., and Valley, J.W. (1995) Carbon isotope thermometry in marbles of the Adirondack Mountains, New York. Journal of Metamorphic Geology, 13, 577–594.

Lamb, W.M., and Valley, J.W. (1984) Metamorphism of reduced granulites in low-CO_2 vapour-free environment. Nature, 312, 56–58.

McCrea, J.M. (1950) On the isotopic chemistry of carbonates and a paleotemperature scale. Journal of Chemical Physics, 18, 849–857.

Moecher, D.P, Valley, J.W., and Essene, E.J. (1994) Extraction and carbon isotope analysis of CO_2 from scapolite in deep crustal granulites and xenoliths. Geochimica et Cosmochimica Acta, 58, 959–967.

Morrison, J., and Valley, J.W. (1991) Retrograde fluids in granulites; stable isotope evidence of fluid migration. Journal of Geology, 99, 559–570.

Nabelek, P.I. (1991) Stable isotope monitors. In D.M. Kerrick, Ed., Contact Metamorphism, Mineralogical Society of America Reviews in Mineralogy, 26, 395–436.

Newton, R.C. (1986) Fluids of granulite facies metamorphism. In J.V. Walther and B.J. Wood, Eds., Fluid-Rock Interactions during Metamorphism, p. 36–59, Springer, New York.

Newton, R.C., Smith, J.V., and Windley, B. (1980) Carbonic metamorphism, granulites and crustal growth. Nature, 288, 45–52.

Powell, R., and Holland, T.J.B. (1989) An internally consistent thermodynamic dataset with uncertainties and correlations: 3: Applications to geobarometry, worked examples and a computer program. Journal of Metamorphic Geology, 6, 173–204.

Rumble, D. III, and Spear, F.S. (1983) Oxygen-isotope equilibration and permeability enhancement during regional metamorphism. Journal of the Geological Society, London, 140, 619–628.

Sharp, Z.D., O'Neil, J.R., and Essene, E.J. (1988) Oxygen isotope variations in granulite-grade iron formations: constraints on oxygen diffusion and retrograde isotopic exchange. Contributions to Mineralogy and Petrology, 98, 490–501.

Sims, J.R., Dirks, P.H.G.M., Carson, C., and Wilson, C.J.L. (1994) The structural evolution of the Rauer Group, East Antarctica: Mafic dykes as passive markers in a composite Proterozoic terrain. Antarctic Science, 6, 379–394.

Sudicky, E.A., and McLaren, R.G. (1992) The Laplace transformation Galerkin technique for large-scale simulation of mass transport in discretely-fractured porous formations. Water Resources Research, 28, 499–514.

Thost, D.E., Hensen, B.J., and Motoyoshi, Y. (1991) Two-stage decompression in garnet-bearing mafic granulites from Søstrene Island, Prydz Bay, East Antarctica. Journal of Metamorphic Geology, 9, 245–256.

Todd, C.S., and Evans, B.W. (1993) Limited fluid-rock interaction at marble gneiss contacts during Cretaceous granulite-facies metamorphism, Seward Peninsula, Alaska. Contributions to Mineralogy and Petrology, 114, 27–41.

Valley, J.W. (1986) Stable isotope geochemistry of metamorphic rocks. In J.W. Valley, H.P. Taylor, and J.R. O'Neil, Eds., Stable isotopes in high temperature geological processes. Mineralogical Society of America Reviews in Mineralogy, 16, 445–490.

Valley, J.W., Bohlen, S.R., Essene, E.J., and Lamb, W.M. (1990) Metamorphism in the Adirondacks. II. The role of fluids. Journal of Petrology, 31, 555–596.

Zhao, Y., Liu, X., Wang, B., Ren, L., Li., J., and Chen, T. (1992) Geochronology of the late granite in the Larsemann Hills, East Antarctica. In: Y. Yoshida, K. Kaminuma, and K.Shiraishi, Eds. Recent Progress in Antarctic Earth Science, p. 155–161, Terra Scientific Publishing, Tokyo.

Manuscript received March 26, 1996
Manuscript accepted December 9, 1996